A Study of Causal Sets

A Thesis

submitted to

Indian Institute of Science Education and Research Pune
in partial fulfillment of the requirements for the
BS-MS Dual Degree Programme

by

Abhishek V

Indian Institute of Science Education and Research Pune
Dr. Homi Bhabha Road,
Pashan, Pune 411008, INDIA.

April, 2020

Supervisor: Deepak Dhar
© Abhishek V 2020

Certificate

This is to certify that this dissertation entitled A Study of Causal Sets towards the partial fulfilment of the BS-MS dual degree programme at the Indian Institute of Science Education and Research, Pune represents study/work carried out by Abhishek V at Indian Institute of Science Education and Research under the supervision of Deepak Dhar, Professor, Department of Physics , during the academic year 2019-2020.

Deepak Dhar

Committee:

Deepak Dhar

Sreejith GJ

This thesis is dedicated to my parents.

Declaration

I hereby declare that the matter embodied in the report entitled 'A Study of Causal Sets' are the results of the work carried out by me at the Department of Physics, Indian Institute of Science Education and Research, Pune, under the supervision of Deepak Dhar and the same has not been submitted elsewhere for any other degree.

Abhishek V

Acknowledgments

First and foremost, would like to offer my deep and sincere gratitude to my guide, Prof Deepak Dhar, for his invaluable insights and constant support throughout this project, and many others as well during my stay in IISER. I would also like to thank Prof Sreejith GJ and Prof Sumati Surya for their valuable inputs. This work would not have been possible if not for the moral support of my parents and my brother (and the canine member of our household, Mothi), who have weathered many a storm during my stay here, and yet, have offered nothing but positivity and encouragement. I would also like to express my boundless gratitude to all my friends for making sure that I will cherish these years as one of the best periods of my life.

x

Contents

List of Figures

List of Tables

Abstract

In this thesis we study some aspects of causal set theory. In Chapter 1 we briefly motivate this theory, outline some important results and describe some of the work that has been in done this field so far. In Chapter 2 we outline the various definitions and terminologies that will be used throughout the thesis. In Chapter 3 we study the Poisson sprinkling method to generate causal sets and study various properties of such causets, primarily the volume-diameter scaling to estimate the causal set dimension. In Chapter 4 we try to generate causets in the form of a layered, directed graph and try to find their causal set dimension. In Chapter 5 we will use the tilted square lattice as the basic framework of our causal set, and study how rewirings and percolation affect its various properties. In Chapter 6 we summarise our results and outline how we can build upon this work.

Chapter 1

Introduction

1.1 A brief account of earlier work on on Causal Set Theory

Achieving a theory of quantum gravity has been one of the most important goals of physics for the last few decades, and a significant amount of work has been done to this end[1]. One of the theories that attempts to tackle this problem is the *causal set theory*[2]. This theory posits that spacetime is fundamentally discrete. The most fundamental objects in the spacetime, according to this theory, are events and causal links. What we perceive as coordinates are emergent. What we are essentially doing is transforming the kinematics of our system from a manifold and a metric $(\mathcal{M}, g_{ab})$, to a partially ordered set, with an ordering relation $(C, \prec)$.

It has been shown by Hawking *et al.*[3, 4] that, in 4 dimensions, the metric is almost completely determined by the causal structure of the spacetime, sans a local volume element (which is a single scalar). In the words of Finkelstein[4], the causal structure (in 4 dimensions) determines $9/10^{\text{th}}$ of the metric. This is because a $(3+1)d$ spacetime metric has 10 independent degrees of freedom, and the causal structure of spacetime determines all of them, sans a conformal factor. The fundamental nature of the causal structure of spacetime was strengthened by Zeeman in his paper[5] entitled 'Causality implies the Lorentz Group', where he goes on to define a *chronological automorphism*, and proves that the group of these

automorphisms is isomorphic to the Lorentz group.

However, we must still determine what is to become of the remaining '1/10$^{\text{th}}$' of the metric. One way to do this is to demand that spacetime be *locally finite*[6], wherein we demand that there be only a finite number of spacetime elements (or events) in a finite spacetime volume. We can thus obtain discreteness in the poset which represents spacetime. We also demand that, on an average, these points are separated by a distance of order Planck length. Now we can replace the notion of a continuous volume of any interval in spacetime with the notion of a discrete volume, which is simply by the number of events in the interval. We now have a theory of spacetime wherein we have a partially ordered set $(C, \prec)$ as the dynamical variables, as opposed to a manifold and a metric $(\mathcal{M}, g_{\mu\nu})$. This partially ordered set is called a *causal set*, or more simply, a *causet*.

One way to construct these causets directly from continuous spacetime by 'sprinkling' points in continuous space such that the number of points in a given volume of spacetime follows a Poisson distribution (keeping in mind that the average distance between points is of order Planck length), and assigning causal links between these sprinkled points in accordance with the causal structure of the underlying spacetime. However, we would like to develop a method to generate such causets by using methods other than this because this uses a manifold like spacetime as a crutch, and we want to eventually show that what we need is a causal set and "manifold-ness" is emergent. There has been some work done in this regard, like transitive percolation[7, 8], and there have also been attempts to see whether the causets generated this way have other properties of spacetime like Lorentz invariance[9] on a large scale, and so on.

1.2 Scope of this thesis

In this thesis we aim to introduce a few concepts of causal set theory (or CST) and study some aspects of it. Here we do not even attempt to answer many of the problem in CST, and will stick to only a few. For a more detailed account of the work that has been done in this field please refer to this review article[10] by Surya. The following are the broad topics covered in the thesis:

- Definition of a causal set, and few other important concepts like faithful embedding,

causal set dimension, diameter etc.

- Enumeration of causal sets that are constructed using some toy models

- Determination of the probabilities of occurrences of various topologies in causets generated using a method called Poisson sprinkling, and coming up with an analytical explanation for the same

- Generating causets using Poisson sprinkling and studying the volume *vs.* diameter relationships of such causets and their subcausets

- Examination of the abundances of subcausets of various diameters and volumes within a causet

- Development of a different method for generation of causets (much like the transitive percolation method) where we have layered graphs

- Performing rewirings and percolation on these graphs and see how these influence various properties of the causet

- A study of different properties of the graphs generated this way and see if we can somehow reproduce at least some of the properties of the causets that we obtained by Poisson sprinkling.

The quantity of interest in this thesis is the dimension of causets, which we will define by studying volume *vs.* diameter relationships. An important disclaimer is that we do not aim for the layered-graph causal set to completely mimic spacetime, but to mimic some properties in some limits.

All simulations in this project were run on FORTRAN using the *gfortran* compiler. Graphs were plotted using Grace and Python 3. Numerical calculations were done using Wolfram Mathematica.

Chapter 2

Preliminaries

2.1 General definitions

Here we shall define certain terms and clarify certain concepts that will be used throughout the thesis, and also make note of conventions used.

2.1.1 Causal sets

Let us first define what a causal set is. A causal set is a partially ordered set where the partial ordering relationship between two elements is determined by whether they are causally linked by the causal structure of spacetime. In a causal set, $a \prec b$ if and only if a exists in the past light-cone of b in spacetime.

A partially ordered set is a set with S with any partial ordering $\prec$ where any two elements $a, b \in S$ can either be related ($a \prec b$ or $b \prec a$) or unrelated ($a \nprec b$ and $b \nprec a$). The partial ordering relation $\prec$ must satisfy the following criteria:

- *Antisymmetry:* $a \prec b \Rightarrow b \nprec a$

- *Transitivity:* $a \prec b$ and $b \prec c$ together imply $a \prec c$

- *Non-circularity:* $a \prec b$ and $b \prec a \Rightarrow a = b$

2.1.2 Faithful embedding

Consider a Hausdorff, paracompact manifold $\mathcal{M}$ with a globally hyperbolic, Lorentzian, smooth metric g_{ab} (or simply, a manifold and metric which resembles the real spacetime that we see). Consider a map $\phi : S \longrightarrow \mathcal{M}$ from a causal set $C = (S, \prec)$ to a spacetime manifold $(\mathcal{M}, g_{ab})$. It is called a *conformal embedding* if $x \prec y \iff \phi(x) \prec J^-(\phi(y)); \forall x, y \in S$ (J^+ and J^- denote *to the future of* and *to the past of* respectively). The map is called a faithful embedding if it satisfies two other criteria:

1. The probability of having n points mapped into an Alexandrov interval of spacetime volume V is
$$P(n) = \frac{(\rho V)^n e^{-\rho V}}{n!}$$

2. The mean spacing between points ($\rho^{\frac{1}{d}}$ in d dimensions) has to be greater than than the lengthscale over which continuum geometry varies.

2.1.3 Hasse Diagrams

These are diagrams used to represent partially ordered sets (or *posets*). As causal sets are essentially partially ordered sets, Hasse diagrams give us a good way to represent them as well. We can draw these diagrams with the following rules:

- Each element in the causal set is denoted by a point

- Two points x and y are connected by a line if and only if $x \prec y$ in the causal set and there is no z such that $x \prec z \prec y$

Each causal set has a unique Hasse diagram corresponding to it and vice versa.

Given that this is a partial ordering, this is a representation of the poset which resembles a directed, transitive graph. As a convention, we shall adopt the downward direction to represent all causets henceforth. Also, $x \prec y$ in any causet means that event x can causally influence event y.

2.2 Definitions pertaining to causal set dimension

Given that we are going to investigate causal set dimension in some detail in this thesis it becomes pertinent to discuss few of the ideas that we will be using to do so. As the causal sets that we construct in the form of a poset, and therefore, in the form of a directed graph, will in genera have a fractal dimension, we can have various measures of dimension which can be used.

2.2.1 Volume of a causet

As it has been indicated before, the volume of a causet is simply its cardinality. In this thesis we will be examining intervals in causal sets so we shall define it in detail here.

Consider a causal set $C = (S, \prec)$. Consider two points $x, y \in S$ such that $x \prec y$. The volume of the interval between x and y is the cardinality of the set $I[x, y]$ where $I[x, y]$ is $J^+(x) \cap J^-(y)$. As we have alluded to before, $J^+(x) = \{z : z \in S, x \prec z\}$ and $J^-(x) = \{z : z \in S, z \prec x\}$.

2.2.2 Diameter of a causet

Firstly, we shall define what a *path* is, and move ahead from there. A path P between any two points $x, y \in S$ (and $x \prec y$), is a set of causally linked elements with x as its past endpoint and y as its future endpoint **and** there exists no element z that is comparable to *all* elements in P such that $x \prec z \prec y$. The length of any path P is the cardinality of P.

The diameter of a causet is is defined to be the *length* of the longest possible *path* that can be traced out in the causet. Suppose our causet has a past endpoint x and a future endpoint y, the diameter of the causet is the length of the longest path that joins x to y. This longest path, in fact, is a timelike geodesic between these two events. This directly corresponds to the notion of timelike geodesic in continuous spacetime, where we find said geodesics by extremising proper time.

It has been shown[11, 12] that for any interval $I[x, y]$ of a causal set (constructed by

sprinkling) of discrete volume ρV, the length L of the longest chain satisfies $L(\rho V)^{1/d} \to m_d$ in probability, where m_d is some constant that depends on the dimension of the Minkowski space. For $d \geq 3$, we have the following bounds:

$$1.77 \leq m_d \leq 2.62 \tag{2.1}$$

We also know that $m_2 = 2$.

2.2.3 Dimension of a causet

The dimension of a causet can be defined in a variety of ways, given that the causet itself will in general have a fractal dimension. In this thesis, we will use the volume-diameter scaling to define our dimension (we will define this rigorously in this section). However, there exist other possible definitions of causal set dimensions (like the mid-point scaling dimension, the Myrheim-Meyer dimension etc, and one can find these definitions in the thesis by Rideout[8].

In $d-$dimensional Minkowski space, the spacetime volume between two events which are separated by proper time T has spacetime volume

$$V_d(T) = \frac{2V_{d-1}}{d}\left(\frac{T}{2}\right)^d = \frac{2\pi^{(d-1)/2}}{((d-1)/2)!d}\left(\frac{T}{2}\right)^d \tag{2.2}$$

Though this definition is for continuous spacetime, it can be extended to causal sets as well because we have precisely defined what volumes and diameters of causal sets are. However, there is the caveat of how we do not know how to translate the casual set length L to the proper time T, as we do not know m_d, in general. However, for $d = 2$, which is what we will be examining in this thesis, m_2 is well defined and we can go ahead.

It must be noted that we do not insist on the prefactor being the same as what we see here for the causal sets that we will generate using various rules. All we want to see is how the volume of a causal set grows as a function of its diameter. Essentially, we will have an expression for the volume of a causet as a function of its diameter and we will find $\log(V)$. The coefficient of $\log(d)$ in this expression is what we define to be the dimension of the causet.

2.3 A few simple examples

In CST, different posets occur with different probabilities, and all allowed posets will get assigned non-zero weight by the theory being considered. We will try to enumerate causets which are subject to some constraints. Here are few simple examples:
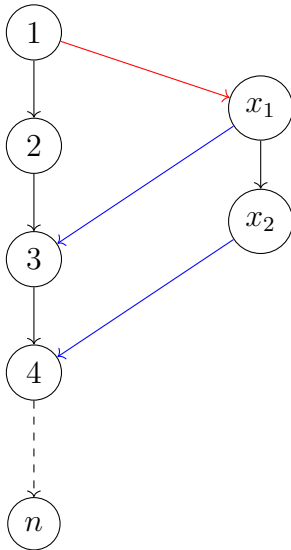
Case 1
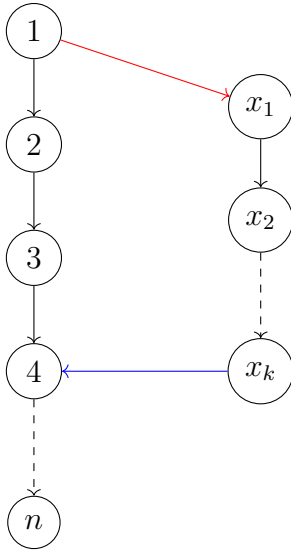
We enumerate the non-trivial causets formed by linking two chains, one of length n and the other of length k when the tips of the "side-chain" is connected to the main chain with one incoming and one outgoing edge.

The number of such causets is $\dfrac{n!k!}{2}(n-1)(n-2)$

Case 2

We enumerate the non-trivial causets formed by linking a of length n and another of length 2 where the topmost tip of the "side-chain" is connected to the main chain by *two* edges (one incoming and one outgoing) and the bottom-most tip by one edge (one outgoing).

The number of such causets is $\dfrac{n!}{2}(n-1)(n-2)\left(n-\dfrac{3}{2}\right)$

It is important to note that while we can construct many such partial orderings, it is very hard to obtain partial orderings that look like spacetime-like. In fact, Kleitman and Rothschild[13] showed that most random partial orderings of n elements have a three layered structure similar to that of a tripartite graph, and the number of such posets are bounded by:

$$\frac{n^2}{4}\log(2) \leq \log(N(n)) \leq \frac{n^2}{4}\log(2) + An^{3/2}\log(n)$$

where $N(n)$ is the total number of posets that can be formed with n elements. These tripartite graphs do not represent spacetime whatsoever, hence we need to device some other method to generate/enumerate posets that look like spacetime.
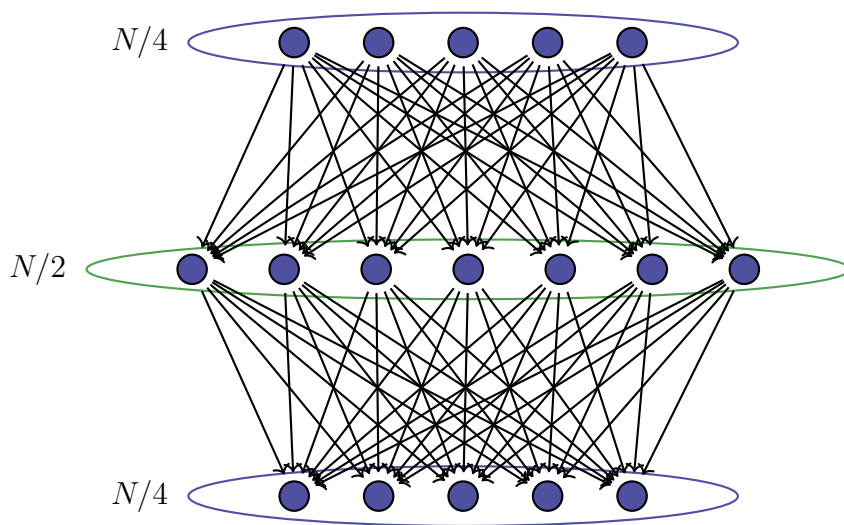

Figure 2.1: A typical Kleitman-Rothschild poset of N elements. They organise themselves into three layered posets where the outer layers have $\sim N/4$ elements each and the middle layer has $\sim N/2$ elements (the actual number of nodes in this figure are for illustrative purposes only).

Chapter 3

Poisson sprinkling to generate causets

As previously mentioned, one way of generating causets is to sprinkle points into spacetime such that

1. Given a density of sprinkling ρ, the probability of finding n points in a volume V of spacetime is given by

$$P(n) = \frac{(\rho V)^n}{n!} e^{-\rho V} \tag{3.1}$$

2. The density of points is fixed to a good extent by insisting that the average distance between two events in this causal set is lesser that some length-scale λ where the scale at which spacetime geometry varies is $\gg \lambda$. We can consider $\lambda \sim l_P$, the Planck length.

In Minkowski spacetime this is simply uniform sprinkling of points. What one can do is to call two random numbers to be our x and y coordinates. We will, however, do all our sprinkling in a *causal diamond*, which is simply the spacetime interval between two events (in $(1+1)d$) Minkowski spacetime.
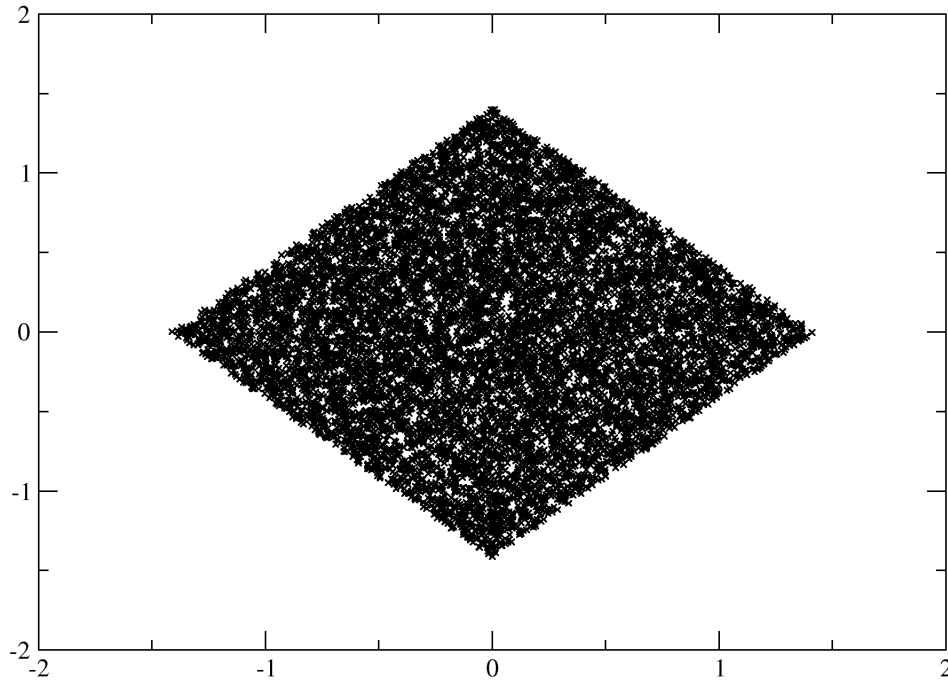
Figure 3.1: 10^4 points uniformly sprinkled in a $(1+1)d$ Minkowski causal diamond

3.1 Probability of finding different topologies

One interesting question that we can study here is this: if we sprinkle n points in a Minkowski diamond, they can fall into different topological configurations. The aim is to determine what is the probability of getting a particular kind of configuration given that n points were sprinkled. Simulations for $n = 2, 3, 4$ were run. In the following tables, the left-hand column shows the structure of the causal set, and the right-hand column contains rational fraction approximations of the data that we obtained from simulations.

Table 3.1: $n = 2$, simulation. We can see 2 distinct topological configurations.

	$\dfrac{1}{2!}$
	$\dfrac{1}{2!}$

12

Table 3.2: $n = 3$, simulation. We can see five distinct topological configurations
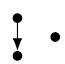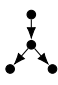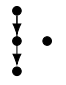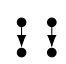
	$\dfrac{1}{3!}$
	$\dfrac{2}{3!}$
	$\dfrac{1}{3!}$
	$\dfrac{1}{3!}$
	$\dfrac{1}{3!}$

Table 3.3: $n = 4$, simulations. We can see sixteen distinct topological configurations.

	$\dfrac{3}{4!}$		$\dfrac{2}{4!}$		$\dfrac{1}{4!}$		$\dfrac{1}{4!}$
	$\dfrac{2}{4!}$		$\dfrac{2}{4!}$		$\dfrac{1}{4!}$		$\dfrac{1}{4!}$
	$\dfrac{2}{4!}$		$\dfrac{2}{4!}$		$\dfrac{1}{4!}$		$\dfrac{1}{4!}$
	$\dfrac{2}{4!}$		$\dfrac{1}{4!}$		$\dfrac{1}{4!}$		$\dfrac{1}{4!}$

In principle, it is possible to write down the various topological configurations for any n number of points. However, the number of such configurations grow very fast for us to do it. For example, if we want to consider the 5 points being sprinkled, we trivially have $3 \cdot 16 - 3 = 45$ configurations: one where you have the new element unrelated to none of the other four elements, one where the new element is to the past, and another where it is to the future of all the remaining 4 elements (the 3 is subtracted because there are a few repetitions when we follow these scheme). There will be more topologies than this, and it becomes tedious to list them all out for larger and larger n.

It is possible to obtain these exact probabilities we saw in the preceding tables analytically. We can show that sprinkling in 2-d Minkowski spacetime are isomorphic to a random permutation in the following way:

1. Consider a permutation $\boldsymbol{\pi}_i$ of n numbers, with $1 \leq i \leq n!$, where $\boldsymbol{\pi}_i = (\pi_i(1), \pi_i(2), \ldots, \pi_i(n))$.

2. Let us label n points as the first n natural numbers

3. We say that two points x, y are connected with $x \prec y \iff$

   - $x < y$, and
   - $\pi_i(x) < \pi_i(y)$

We can hence generate causets from permutations using this scheme. Coming back to the probability of finding different kinds of topologies in causets, we can think of random sprinkling of n points as generating a random permutation of n numbers. Here, each permutation occurs with a probability of $1/n!$. However, different permutations can give rise to the same topologies. For example, consider the poset

Figure 3.2: A causet with 4 elements

Now the permutations 3421, 4312 and 4231 correspond to this causet. As three of the 4! permutations correspond to this topology and each of them occur with probability $1/n!$, the probability of occurrence of this topology when 4 points are sprinkled is $3/n!$.

14

We can generalise this as:

$$\text{Probability of finding a given topological configuration} = \frac{\text{Number of permutations which give the configuration}}{\text{Total number of permutations}} \quad (3.2)$$

3.2 Volume *vs* Diameter characteristics

We generated causets using various rules to estimate how their volumes vary with change in their diameters, and vice versa. Simulations where we generated causets by sprinkling points into a 'causal diamond' (which is the spacetime interval between two timelike separated events) were performed and volume *vs* diameter behaviour was studied.

3.2.1 Varying V

A fixed number of points were sprinkled into a causal diamond, thereby fixing the volume. Then, the longest chain in the graph obtained by sprinkling was found and its length was defined to be the diameter of the causet. This procedure was repeated multiple times for the same volume to obtain the variance in diameter for a given volume, and then the volume was also varied to express the average diameter as a function of volume.
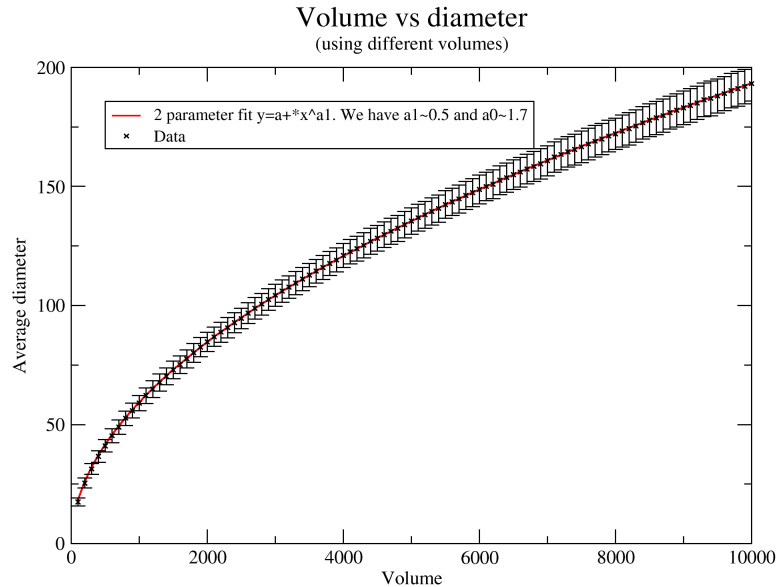
Figure 3.3: d (diameter of the causal set) vs V (Volume): fixed V

We can see that volume goes as mean diameter to the power 2, with some small error.

3.2.2 Calculating subcauset volumes

Another way to study the volume vs diameter relationships are to generate a single causet and look at all its subcausets and study their volume *vs* diameter relationship. We can also study other properties of the causet, like what is the distribution of the causet volume given a diameter, what are the number of causets of a given diameter, and so on. This scheme is similar to the previous one, except the top and bottom points of the causal diamond are occupied as we use these points to define the subcauset.
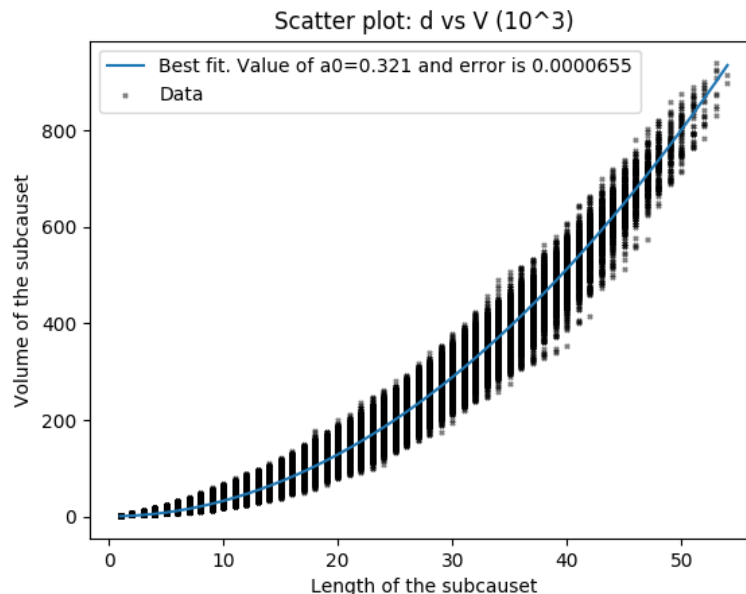
Figure 3.4: A scatter plot of d (diameter of the causal set) vs V (Volume): all the volumes for different values of d have been plotted

As we can see, there is a distribution of volumes about the mean volume for a given diameter. The distribution appears to become thinner towards the high diameter end of the causet simply because the number of high diameter subcausets of a given causet becomes smaller and smaller, with increase in diameter, and becomes something to the order of 1 as the diameter approaches the diameter of the causet itself.

Another quantity that can be studied is the distribution of of the causet volumes about the mean, for a given diameter.
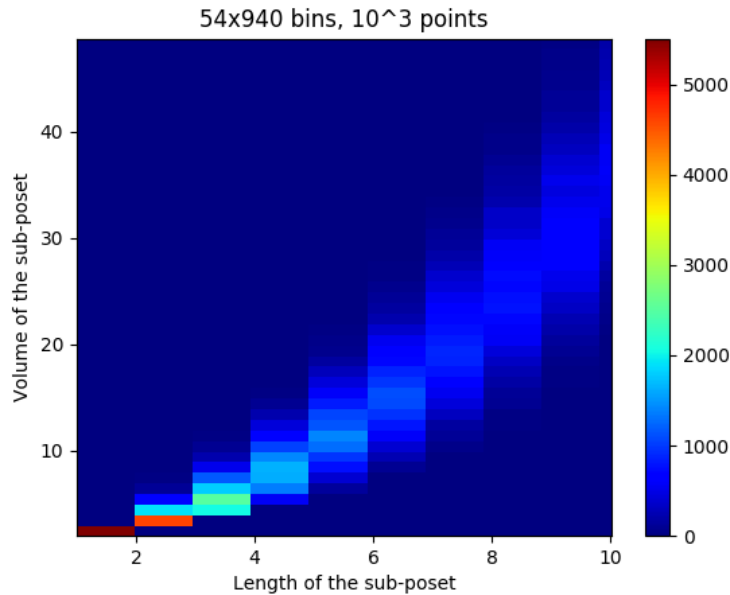
Figure 3.5: d vs V: heat plot, zoomed in. We have some idea about the density of data points around the fit-curve

As we can see from the heat plot, the low diameter end of the figure has a high density of points and it becomes sparser as we move to higher diameters. The reason for this is twofold: the number of very small diameter subcausets is large compared to those of vary large diameters, and the number of possible volumes that a small diameter causet can have is also quite constrained while compared to those of the subcausets with larger diameters.

The following page has a plot of how the number of subcausets of a given diameter d vary with increase in d. Given that we have a finite system, we will have finite size effects, which we can take into account. The number of length d subcausets would increase somewhat linearly initially, and then the linear growth will become slower and slower, and it will start decreasing after the causet can no longer accommodate subcausets of such large diameters.
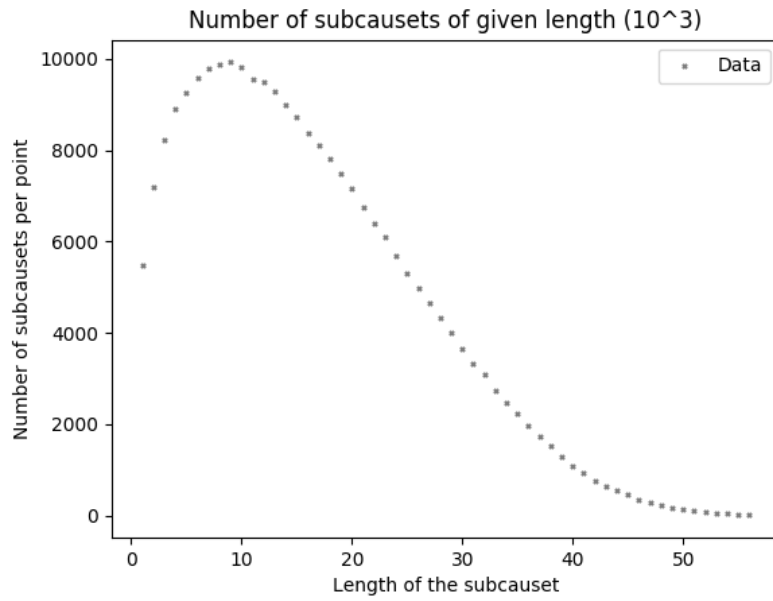
Figure 3.6: Number of subcausets of a given diameter d vs d

We can also study the volume distribution of causets of a given diameter.
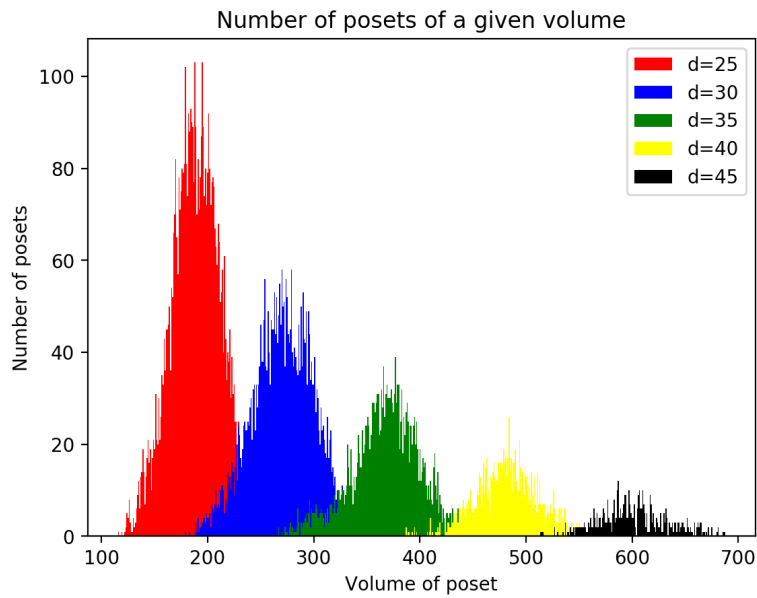
Figure 3.7: The distribution of volumes of causets of a given diameter

All these properties of causets generated from Poisson sprinkling will aid us while we try to produce causets that look like Poisson sprinkled causets from different schemes.

3.3 Number of subcausets of a given diameter

Given a uniform random sprinkling of points in an Alexandrov interval, we would like to know the number of subcausets of a given diameter in the interval. This is an interesting quantity to study because, as we have mentioned earlier, we would want to develop a method of generating causets without assuming an a priori known continuum measure. As we know that most random partial orderings are Kleitman-Rothschild like 3 layered partial orderings, we would like to have a scheme where we attach an energy cost to causets that look like n-partite graphs. There has been some work done[14] which points at the fact the this energy cost might depend on the *abundance* (i.e. the number of subcausets of a given diameter in a causet) of subcausets of various diameters.

We will study what is the behaviour of the number of subcausets of a given length as we increase the number of points sprinkled.

3.3.1 Simulations
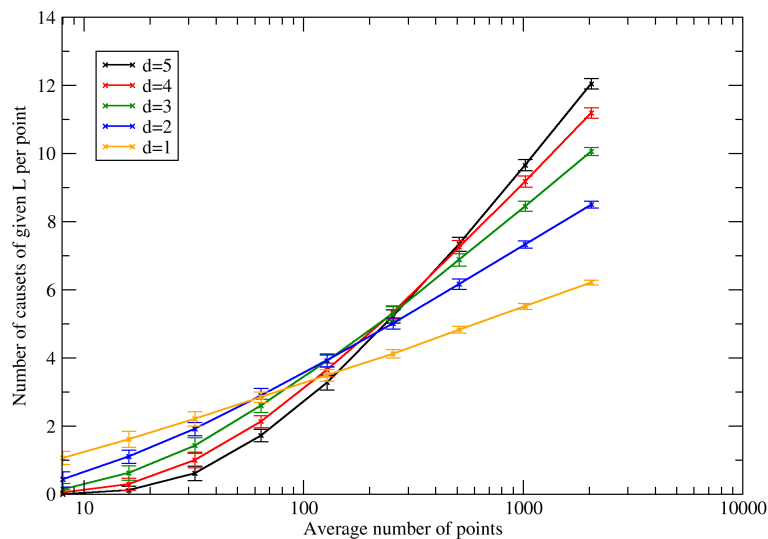
Figure 3.8: Number of subcausets of given diameter d vs number of sprinkled points n

19

As expected, we can see that the number of subcausets with a given diameter grows as the number of points sprinkled increases. Also we see that thought the subcausets of larger diameters are initially outnumbered by the number of the subcausets of smaller diameters, we see that the former overshoots the latter eventually.

3.3.2 Analytical calculation

It is possible to formulate an analytical solution for this problem, and actually arrive at a closed-form solution for the $d = 1$ case.

Consider a causal diamond of side L. We will sprinkle points in this diamond with density ρ. Now for a subcauset of diameter d to exist within this causal diamond a spacetime volume interval between two events (say $\boldsymbol{x}, \boldsymbol{y}$ to have points in them sprinkled such that the longest chain joining x and y is of length d. This means that the longest increasing subsequence[1] in the permutation that represents the causet must be of length d. Say we have m points sprinkled in the spacetime interval between $(\boldsymbol{x}, \boldsymbol{y})$, and the probability of it having a longest increasing subsequence of length d is $P_m(d)$. We know that the volume of spacetime is invariant under Lorentz transformations and that the volume is simply that of the rectangle traced out by null lines from the two events. The expression for the expected number of subcausets of diameter d is given by

$$S_d(\rho, L) = \sum_{m=0}^{\infty} \int_{x_1=0}^{L} \int_{x_2=0}^{L} \int_{y_1=0}^{x1} \int_{y_1=0}^{x2} \rho P_m(d) \frac{(\rho(x_2 - y_2)(x_1 - y_1))^m}{m!} e^{-\rho(x_2-y_2)(x_1-y_1)} \qquad (3.3)$$

where $\boldsymbol{x} = (x_1, x_2)$ and $\boldsymbol{y} = (y_1, y_2)$ are the coordinates of the events in the light cone coordinate system.

The expression for $P_m(d)$ is, in essence, the famed longest increasing subsequence problem[15]. Also known as Ulam-Hammersely problem[16, 17], it is hard problem which has not been solved. There are few results known here, which we can discuss in the context of Poisson sprinkling. say we are considering the set of all permutations S_n, and σ_i's are its elements. Let $L_n(\sigma)$ be the length of longest increasing subsequence in the permutation of n elements, σ. Now we can define the average length of a sequence given the sprinkling of n

---

[1]The longest increasing subsequence of any permutation $\boldsymbol{\sigma} = (\sigma_1, \sigma_2, \ldots, \sigma_n)$ is the longest possible sequence $(\sigma_{i_1} < \sigma_{i_2} < \cdots < \sigma_{i_k})$ that can be constructed such that $1 \leq i_1 < i_2 < \cdots < i_k \leq n$. k is the length of this sequence.

points as $l_n = \frac{1}{n!} \sum_{\sigma \in S_n} L_n(\sigma)$.There has been work[18] which has determined that for large n we have the expression

$$\lim_{n \to \infty} l_n = 2\sqrt{n} + cn^{1/6} + o(n^{1/6}) \tag{3.4}$$

where $c = -1.77108...$

We can already see that, for large n and on an average, the volume of the causet n goes as $l_n^2/4$, where l_n by definition is is the average diameter of a causet of volume n. We could ascertain this using simulations (see Figures 3.3 and 3.4), and also could obtain the factor $1/4$ with d^2, where d was the diameter of the causet.

Asymptotic probability distributions of L_n (that is, $P_n(d)$ as $n \to \infty$) have been found[18] as well. However, for our problem, we are considering small diameter causets, and the large n limit will not work here. The maximum diameter of subcausets that we are considering in our simulations is 5, so they are by no means high volume subcausets. So we cannot use these distributions to help us with our analytical solutions.

However, we can proceed for the $d = 1$ case, because here we just need the probability of finding *no* point within the spacetime interval demarcated by the events $\boldsymbol{x}, \boldsymbol{y}$. This significantly un-clutters the above expression to:

$$S_d(\rho, L) = \int\limits_{x_1=0}^{L} \int\limits_{x_2=0}^{L} \int\limits_{y_1=0}^{x1} \int\limits_{y_1=0}^{x2} \rho e^{-\rho(x_2-y_2)(x_1-y_1)} \tag{3.5}$$

This can be solved to yield:

$$S_1(n) = \frac{2(1 - e^{-n} + \Gamma_e + (\Gamma_e - 2)n + (1 + n)[\Gamma(0, n) + \log(n)])}{n} \tag{3.6}$$

where $S_n(d)$ is the number of $d = 1$ subcausets, $\Gamma(a, b)$ is the incomplete gamma function, and Γ_e is the Euler gamma constant. ρ and L appear in this expression only as ρL^2, so we can replace it by the expected number of points sprinkled in the causal diamond, n.

For very large n, this expression quite simply reduces to

$$S_1(n) \sim 2\log(n) - 2.845 + O(\frac{1}{n}) \tag{3.7}$$

We can verify that this expression agrees very well with our simulation for $d = 1$ causets:
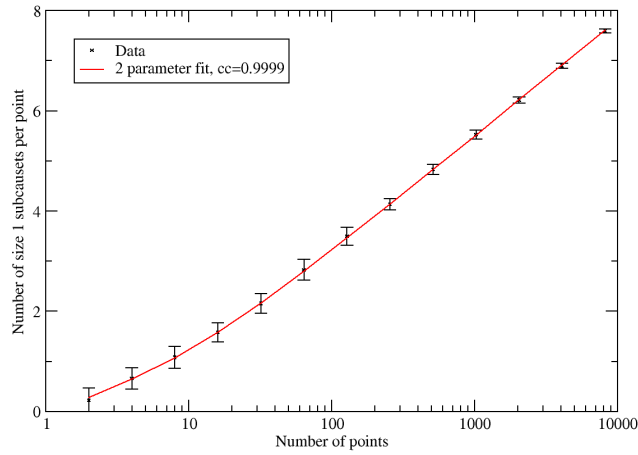
Figure 3.9: Number of subcausets of $d = 1$ (data and analytical solution) vs number of sprinkled points n. The fit is of the form $A_0 \log(n) + A_1$.

A five parameter fit was also done where the parameters of fit agreed with those from theoretical calculations to a minimum of three decimal places.

Chapter 4

Layered posets 1

So far we have studied causets that are generated by Poisson sprinkling into Minkowski spacetime. However, we would prefer to not rely on spacetime itself to provide the geometry for our causal sets, and we would want to generate causal sets that look like spacetime. This becomes a rather difficult task, given that the vast majority of partially ordered sets resemble the Kleitman-Rothschild like n-partite graphs. In this chapter, we will discuss some schemes to generate causal sets, and study whether they are similar to the 'manifold-like' causal sets generated by Poisson sprinkling.

4.1   Layered posets using random derangements

Here we start off with the elements of our poset arranged in layers. In the simulation, there were 100 layers, and each layer had 100 points. Henceforth, we will denote the number of layers as l and the number of points in each layer as n. Now, we decided to adopt a scheme where each point is attached to exactly two distinct points below and two distinct points above it. These points themselves are chosen at random. Without loss of generality, one can insist that each point is connected to the point exactly below it and one other point at random. This structure of the graph is essentially isomorphic to $l - 1$ derangements[1].

These derangements were generated by using an algorithm developed by Martinez *et*

---

[1]A derangement is a permutation with no 1-cycles, *i.e.* no element maps to itself.

$al[19]$, to and the volume vs diameter characteristics of these posets were studied.

Volume vs diameter
Random derangements
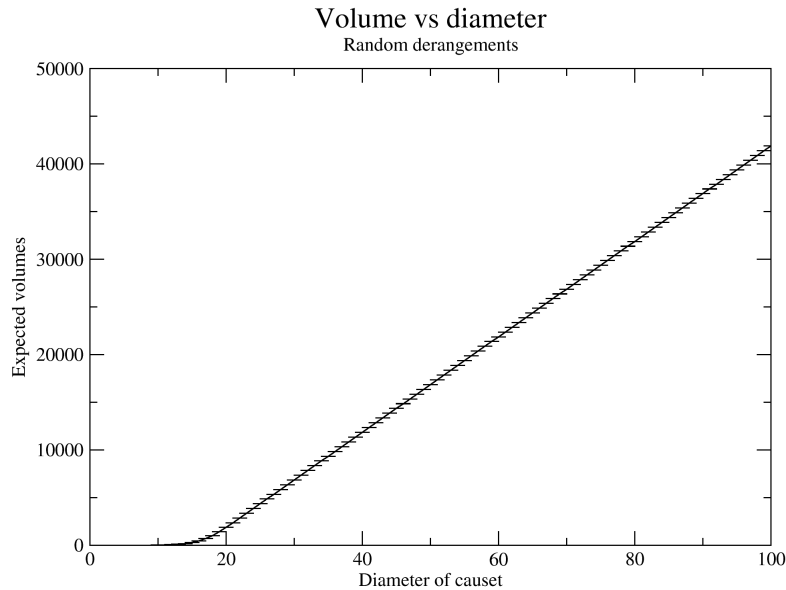
Figure 4.1: V vs d for a layered causet with random attachments. This graph is for $n = 500$ and $l = 100$.

What we can see here is an initial slow linear growth and a faster linear growth later. This is mainly because when we are considering random derangements, the graphs that are generated for large n is roughly tree-like. And volume growth as we have defined it in a tree like graph will be roughly linear in the regions $d \ll \log(n)$ (with slope 1) and $d \gg \log(n)$ (with slope n).

Consider a poset generated by the scheme described above. All subcausets here of diameter 1 will always have a volume 2. We can either have a volume 3 or a volume 4 subcauset of diameter 2. The only way we can have a subcauset of volume 4 when the diameter is 2 is if there is a "looping back" in the graph.
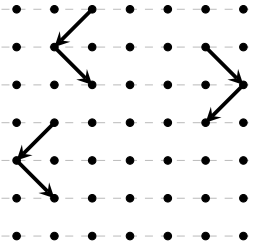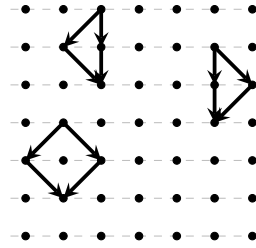
<center>These have volume 3   These have volume 4</center>

Figure 4.2: Subcausets of diameter 2. Each node represents an element of the causet and each edge, a causal link.

The probability of the "looping back" to happen is of order $1/n$ if n points are sprinkled. As the number of points in each layer increase this probability tends to 0. However as the we go down the layers, the number of points are included in each layer increases almost exponentially till all the points in each layer are the descendants of the chosen original point. This roughly divides the volume vs diameter graph into three regions:

1. The initial region (for small d) where the graph looks roughly treelike and we can see linear growth with slope 1 as going to new layer simply adds one point to the subcauset

2. The large d region where 'full percolation' has been achieved and going to the next layer simply adds another entire layer to the subcauset, and not just a single point. This region is also linear and has slope n.

3. The intermediate region which is very short lived which will have a roughly exponential growth such that it joins the two lines of slope 1 and slope n in a smooth way.

This is hardly how we'd expect a spacetime like causet to behave; we would want to see a power-law like growth which indicates some fractal dimension. If we considered a scenario where the $n \to \infty$, then the graph that represents the causal set will always be tree like and all its sub-lattices will exhibit linear growth in volume.

This motivates us to consider graphs that are locally not tree-like (they have loops).

<center>25</center>

4.2 Layered posets with preferential attachments

Given that the random derangement scheme did not yield power-law volume-diameter relationships, we realise that perfectly random derangements are not going to help us represent spacetime. We also saw that for us to see a greater than linear growth in causets we need to have non-tree-like structure locally. We can do this by insisting on looping connections while generating derangements. To do this, let us define a few terms[2] first:

- Each layer is referred to as a *generation.*

- Two points in layer i are called *brothers* if their first common ancestor is in the $(i-1)^{\text{th}}$ layer, and *first-cousins* if their first common ancestor is in the $(i-2)^{\text{th}}$ layer and so on. In general, two points in layer i are called *cousins of order j* if their first common ancestor is from layer $i - (j+1)^3$.

- If two points in layer i are connected downwards to a single point in layer $i+1$, the point they are connected to is called their *common child.*

- Two points in the same layer are said to be *attached* if they have a common child in the next layer.

Instead of generating a random derangement, we can have a scheme wherein we have a few layers of random derangements and then on we can have derangements where brothers and cousins of various orders are preferentially attached. This will ensure the looping which was mentioned earlier, and we can hope to see more complex growth.

However, this scheme runs into a series of problems which makes it quite hard to achieve computationally:

1. The fail rate of the algorithm by which we can generate derangements like the one we described is quite high. For each point we make a list of cousins of various orders and choose one of them for attaching to the said point. This choice[4] is made such that the probability of being attached to a cousin of order i is p_i with $p_i > p_j \forall i < j$. We do this

---

[2]These aren't technical terms, and are just provided for ease of of understanding
[3]Brothers are considered to be cousins of zeroth order
[4]In my simulations I used a scheme where $p_i = p^i$ for some $0 < p < 1$

to ensure that points that are not-so distantly related have a common offspring. This was done for heuristic reasons: if a two points have a common ancestor in the recent past, it is likely that they will have an offspring in the near future as well.

2. Choosing the offspring of each point one point at a time and layer by layer can result in many failures as we reach the end of the layer. The last few points in each layer usually do not have options which are near-cousins. This will result in requiring to restart the assignment of offspring to each point in the layer again. A backtrace algorithm was found to be quite ineffective in alleviating this problem.

3. Though this algorithm has moderate success when the p_i's are very small, and if they have an exit strategy instructing the program to assign any free point in the next layer as an offspring if there is no viability of connection to some first n orders of cousins, it again reflects the linear growth as shown in Figure 4.1. This occurs because (assuming n is very small) is the limited number of choices that exist while scanning through he cousin-list.

4. If the number of orders of cousins considered is higher we again have long range attachments whic will resemble random derangements. This again gives us a behaviour like that of Figure 4.1.

We see that this linear growth of volume is a rather obdurate pattern if we use any scheme similar to the random derangement scheme. Hence, we will have to come up with a new scheme to generate these derangements.

Chapter 5

Layered posets 2: tilted square lattices

5.1   The two offspring method

As described in the previous chapter, we will need to formulate a new way of generating layered posets that can exhibit the power scaling of volumes with respect to diameters. One option that we do have is the tilted square lattice. A tilted square lattice will show a power law behaviour in growth of volume. We derive this analytically in the following way:
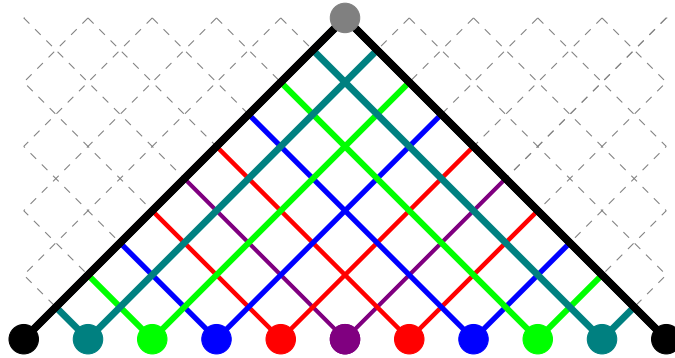

Figure 5.1: $d = 10$ subcausets of tilted square lattice. The bottom boundaries of subcausets of the same volume are shown in the same colour, and the top boundaries are black for all subcausets. The topmost point of each subcauset is the grey node and the bottom-most points are colour-coded.

Consider a causet represented by a tilted square lattice, and let us try and determine the average volume of all its causets of a given diameter d. A causet of diameter d will span through $d+1$ layers of points. Consider some origin point of the subcauset, and consider a 'thin' subcauset (like the one shown in black in Figure 5.1; this subcauset is simply a line of elements). This causet has 'width' 1 and 'length' $d+1$, which will yield a volume of $d+1$. Now, to obtain the volumes of the other causets we increment the width by 1 and decrement the length by 1. Hence the average volume of causets is given by

$$\bar{V}_d = \frac{1}{d+1}\sum_{i=1}^{d+1} i(d+2-i) = \frac{(d+2)(d+3)}{6} \tag{5.1}$$

For large d, $\bar{V}_d \sim d^2/6$ so this does have an asymptotic power law dependence on the diameter of the causet, and dimension of the causet ~ 2. However, this is not a very nice candidate for a causet for the following reasons:

1. This is a purely deterministic grid, and we can see no randomness in this system. We cannot hope to have rotational and Lorentz invariance in a single causet and they are usually satisfied in an ensemble. Randomness is required to generate such an ensemble here.

2. The volume distribution of various posets of a given diameter consists of many peaks as opposed to a gaussian-like distribution as we had seen in the Poisson sprinkling case in Figure 3.7.
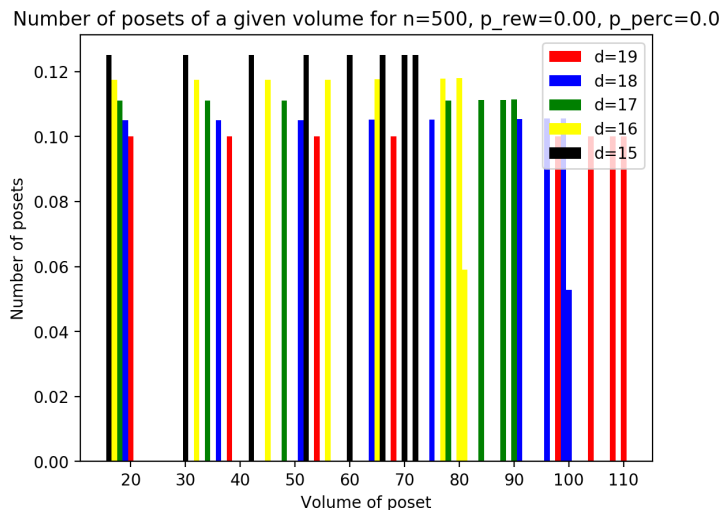

Figure 5.2: Histogram depicting the volume volume distribution of causets with various diameters

We can solve both these problems by introducing rewirings into the system.

5.1.1 Algorithm used for simulation

Just as we saw that random derangements represent random connection between the two layers, a tilted square lattice is represented by a cyclic permutation. In fact we can generate some cyclic permutation $\boldsymbol{\pi}$ (for which I used Sattolo's algorithm[20]). Also, consider the permutation $\boldsymbol{\pi}^*$, which is just the reverse cycle as that of $\boldsymbol{\pi}$[1]. We can use these permutations at random for each layer and we will have a generated a tilted square lattice. Now we can go site by site and call a random number to decide whether we will rewire the bonds to first cousins. We can choose different rules for rewiring, and it not be necessarily to a first cousin. Simulations where we have an energy function which gives us the 'energy cost' of rewiring to cousins of higher orders. We saw that this did not affect the properties of the graphs in a qualitative way, and the rewiring scheme is quite robust in terms of reproducibility of results in different schemes.

An important point to note is that we wanted to preserve coordination number of the points in the graph. So, when there was rewiring there is a swap of bonds, as opposed to a single bond reassignment. However, the coordination number is not preserved, because if one bond is rewired to its first cousin, the other bond that is rewired will either be a bond that already exists as a part of the identity permutation (in this case the coordination number is reduced), or be a rewiring to a fourth order cousin (here the coordination number is preserved).

5.1.2 Volume vs diameter for rewired posets

We can see that curves that correspond to graphs with larger probability of rewiring exhibit more growth than the ones with a smaller probability. This is intuitive, as we will see more 'spreading out' of subcausets within these graphs and they can have greater volumes their same diameter counterparts in the causets with smaller probability of rewiring.

However, after some critical value, the increase in volumes due to rewiring will saturate,

---

[1]This is defined as $\pi^*(i) = j \iff \pi(j) = i$ or if we consider the permutations to be a group, $\boldsymbol{\pi} \circ \boldsymbol{\pi}^* = \mathbb{1}$

as further rewiring does not add any additional randomness to the graph. This is because elements start running out of cousins to get attached to and rewiring attempts start failing. All this is of any use only if we start seeing some randomness in the graphs which we have constructed in this way.
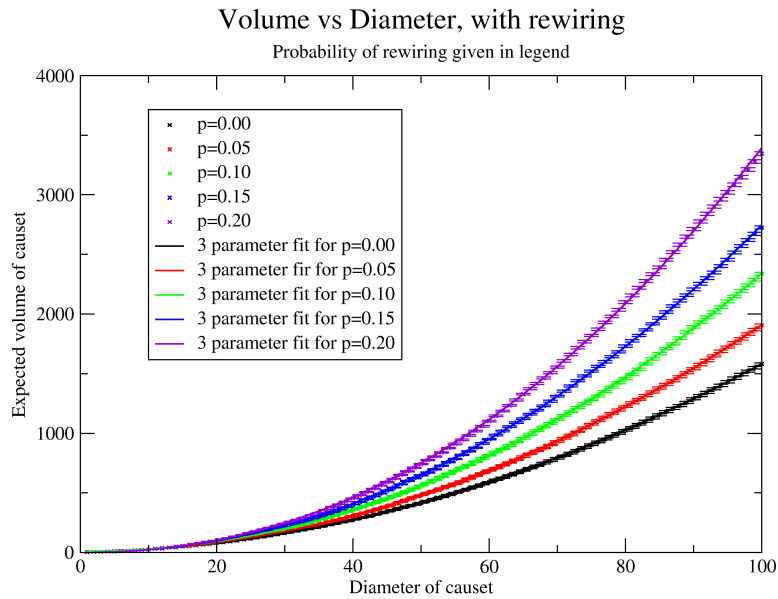
Figure 5.3: Volume vs diameter for a rewired tilted square lattice. The three parameter fit was of the form $y = +a_0 + a_1 x^{a_2}$. $a_2 \sim 2$ for all the given curves.

5.1.3 Volume distribution for various diameters
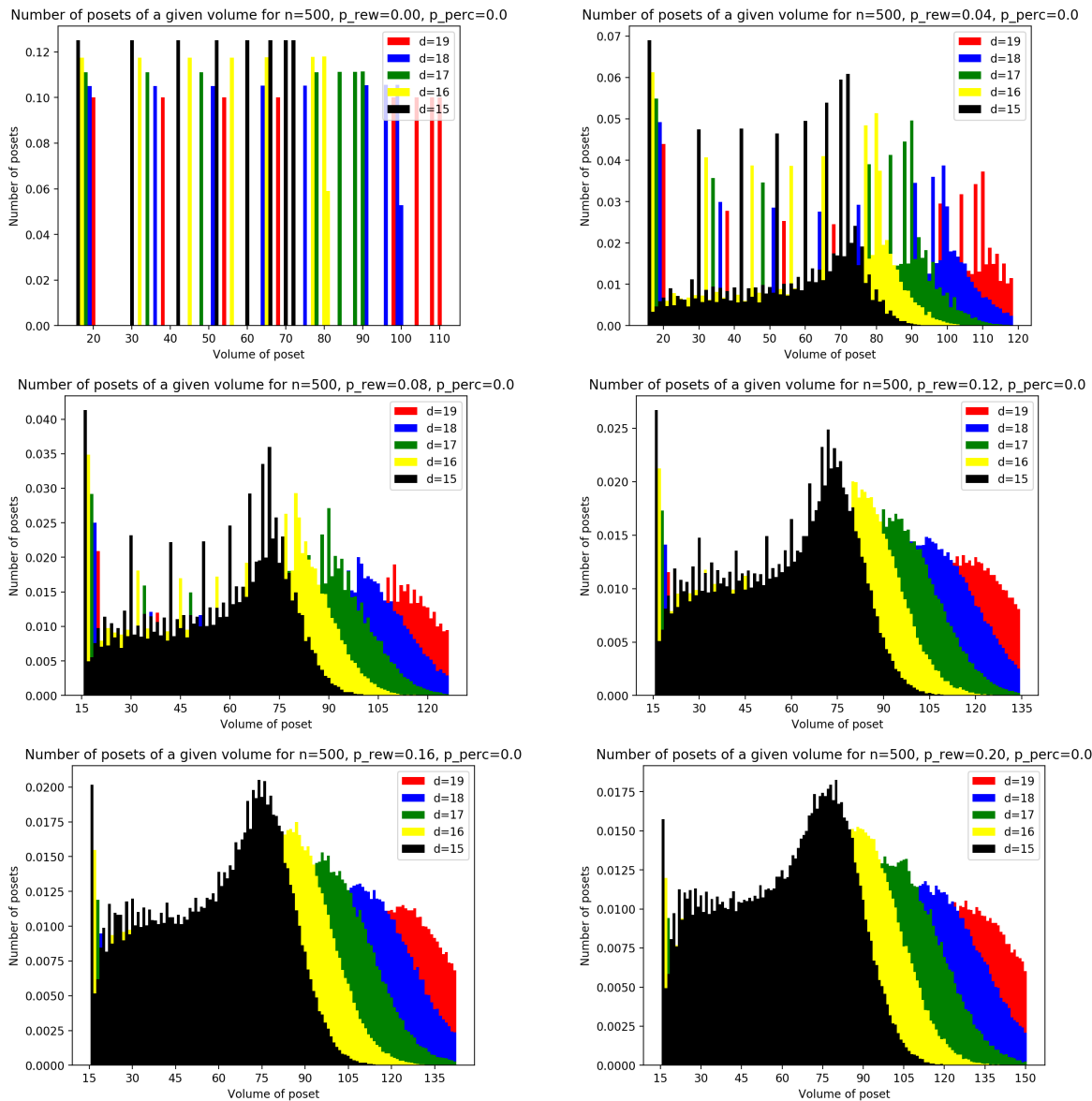
Figure 5.4: Volume distribution of rewired posets of different diameters. We can see the 'spreading out' of the individual volume peaks from $p_{\text{rew}} = 0.00$ to $p_{\text{rew}} = 0.20$

We can infer from these histograms that the deterministic, ordered structure of the causet with $p_{\text{rew}} = 0.00$ quickly disintegrates to give a peak more similar to what we saw in Figure 3.7 (there is another sharp peak in the beginning which we shall address later). These happen because there are additions and deletions to the subcausets that generate the peaks

in the $p_{\mathrm{rew}} = 0.00$ graph. There are a few things that can be said about the rewiring procedure: because these are short range rewirings, the rewirings that affect the volumes of the subcausets will occur near the boundary of the subcauset only. Those in the bulk of the subcauset will not contribute to the additions or deletions of volumes. If we recall the rewiring procedure which had been described previously (and the tilted square lattice and the random connection algorithm before that), we represent the initial tilted square lattice bu an identity permutation *and* by a cyclic permutation. We will rewire only the cyclic permutations here and keep the identity permutations as is. This was done for ease of simulation; doing the other will not give rise to any new observations per se, as these two permutations are not distinguishable if not for the point labels.

In the following diagrams, the thick red lines represent the 'top' edges of the causet and the thick blue lines represent the 'bottom' edges of the causet. We will consider additions and deletions only up to one order in p_{rew} (that is, additions and deletions of volumes that occur with one rewiring only). Additions and deletions due to rewirings can occur only if they happen at the thick red edges because

- Each node on the blue line has two incoming nodes, one of them being a member of the identity permutation. Hence these nodes can never be removed, and nodes cannot be removed from the bulk anyway

- Suppose there is a rewiring to outside the subcauset from inside it across the thick blue edge, the volume that external branch has no way to reconnect with the causet. This branch cannot link back into the causet as, in some sense, the causet is moving 'away' from it as fast as it is approaching the causet (this isn't true if we consider rewiring of order 2 in p_{rew}).

The thin red dotted lines represent the identity permutation, and they will not be rewired. The thin black lines are those that represent the cyclic permutations. Rewirings are indicated by grey lines.

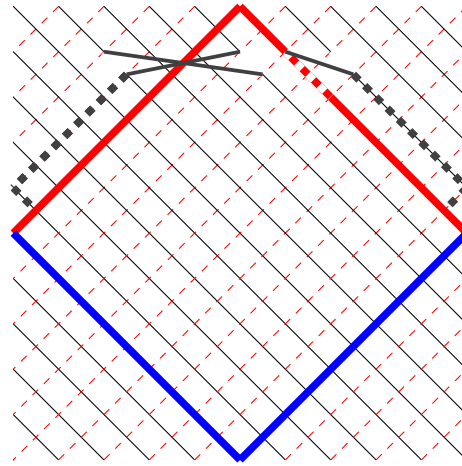1. **Examples of rewirings that result in additions to the volume.**

Figure 5.5: A diagram showing the addition of volumes to a square causet. The dotted gray lines are the additions to the causet and the thick dotted red lines are removed from the causet.

The addition of volume here will be of order $d/4$ for one rewiring at the edge. The number of points viable for this rewiring, which can result in additions is also of order $d/2$. So the additions themselves are of the order $p(d^2/8)$.

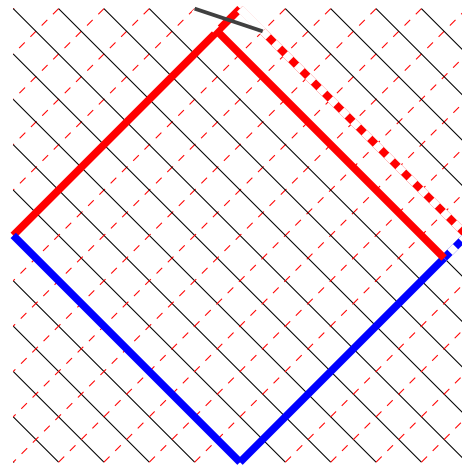2. **Examples of rewirings that result in deletions to the volume.**

Figure 5.6: A diagram showing the deletion of volumes from a square causet. The thick dotted red lines are the deletions from the causet and the thick solid red line is a new boundary of the causet.

The deletion of volume here is of the order $d/2$. However, the number of points which can be rewired to obtain such a deletion is of order 1. So the expected number of deletions to first order in p will be of order $p(d/2)$.

3. **Examples of rewirings that result in no change in volume**
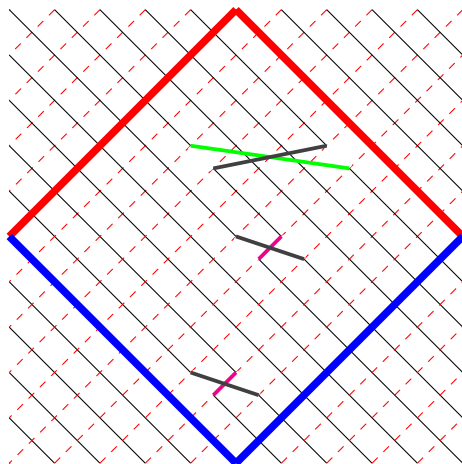

Figure 5.7: A diagram showing rewirings within the bulk of a causet. As expected they do not change the volume of the causet whatsoever.

We can think of rewiring to brothers in the following way: each node lies on an identity permutation line (a red dotted line). This node is attached to a brother by means of a black line which joins an adjacent identity line. A rewiring to a cousin occurs when this black line joins an identity line that is not one, but two places away. As we can see in the causet this rewiring will give another auxiliary rewiring[2]. These rewirings are of two kinds:

1. Sometimes, an element gets attached to its 5th cousin (that is, the element is joined to an identity line 5 places away). This is shown in the colour green in Figure 5.7.

2. At other times, this auxiliary rewiring will be a bond which already exists as an identity link. We can see this as well in two of the rewirings in Figure 5.7, shown in magenta. These bonds are superfluous, and hence can be ignored. Hence, we cannot preserve coordination number if we rewire to first cousins.

---

[2]We have chosen to perform this rewiring in an attempt to preserve coordination number of the element

5.1.4   Volume *vs* probability of rewiring

In the previous section we have seen how rewiring changes the volume distribution of causets of a given diameter. Now we will try and understand how the volume of a causet changes as we change increase the probability of rewiring to first cousins. We must recall that beyond a certain probability we cannot afford to rewire to cousins, as we run out of options. In fact, the probability of successful rewirings plateaus at around $p_{\mathrm{rew}} \sim 0.8$. We can study the volume of high diameter causets and see how they change with increase in probability of rewiring.
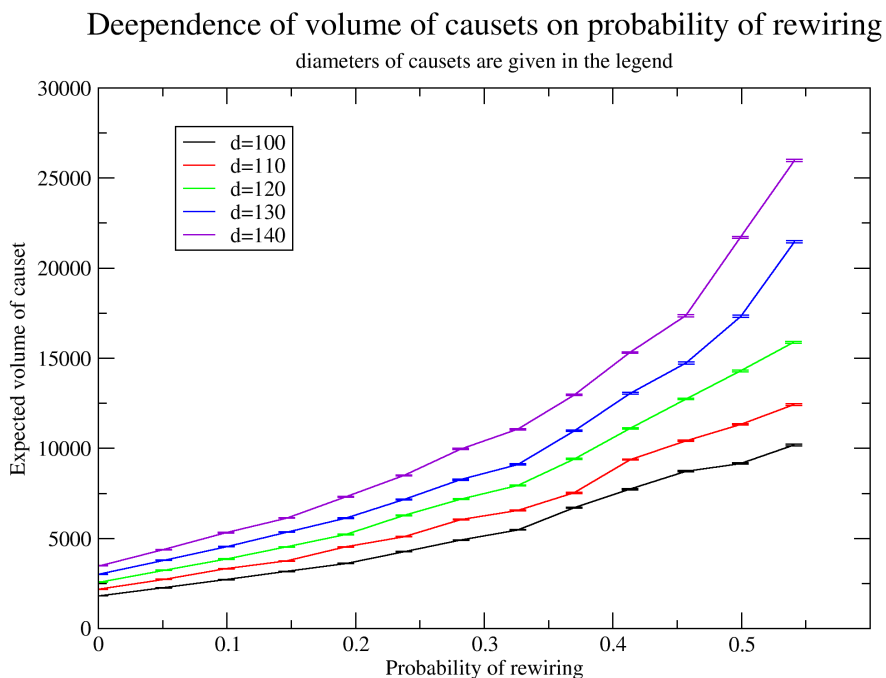
Figure 5.8: Volume *vs* probability of rewiring for different diameters. The simulation was done in a 200 layered causet.

Here we can see the initial region of the graph where the slope goes approximately as d^2. At higher values of p, second order additions become more important as well, hence we see the shoot in volumes. Listing out all the additions and deletions due to two or more rewirings and calculating their probabilities is a hard problem which we shall not attempt.

5.1.5 Percolation on rewired graphs

Though we tried to get a volume distribution of causets similar to that of Figure 3.7, we have found that there is a peak at $V \sim k_2 d^2$, we can also see a peak at $V = d + 1$. This happens because rewirings cannot influence the number of $V = d + 1$ subcausets: we cannot add add or delete elements from a single line, we can only redirect it. The total number of these subcausets remains the same.
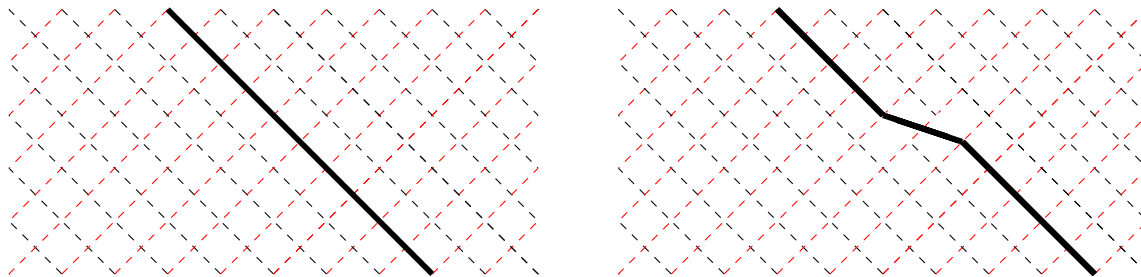

Figure 5.9: $V = d + 1$ subcausets. We can see that the rewiring does not affect the volume of this subcauset, but merely redirects it.

This peak, however, can be diminished by percolating on the graph that has been generated by rewiring. This works because if we remove even a single bond from a 'thin' subcauset (a subcauset whose volume is $d + 1$), the subcauset immediately breaks into two. At higher diameters, we will not find such thin subcausets because it is very improbable for a long chain to exist. While removing bonds, we leave the bonds generated by the identity permutation as they are, as we do not want to have an element with no predecessors. The bonds due to the identity permutation will ensure that this does not happen.
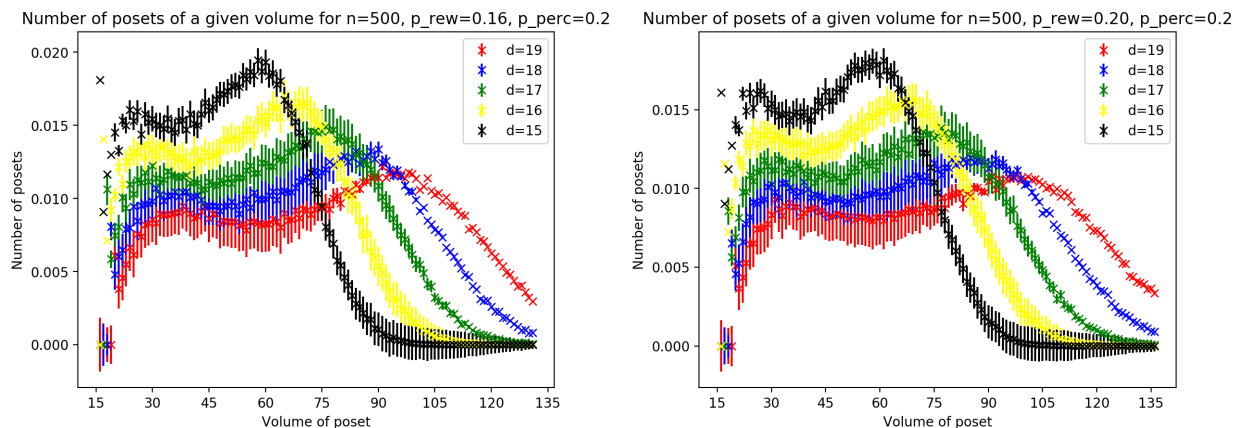

Figure 5.10: Volume frequencies with percolation. $p_{\mathrm{rew}} = 0.16, 0.20$ and $p_{\mathrm{perc}} = 0.2$
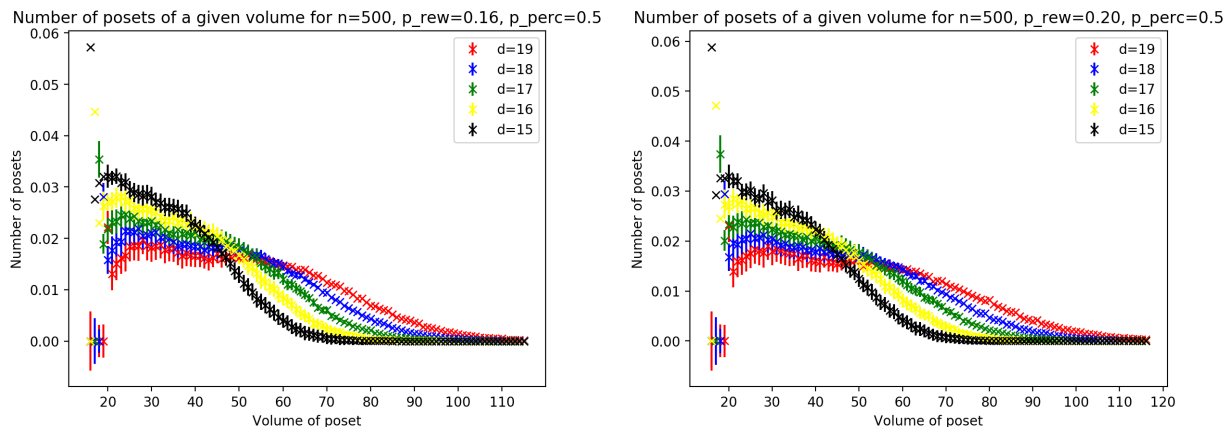
Figure 5.11: Volume frequencies with percolation. $p_{\mathrm{rew}} = 0.16, 0.20$ and $p_{\mathrm{perc}} = 0.5$

This does reduce the prominence of the initial peak, but it isn't enough. Hence we can start over with a different scheme and see if it works.

5.2   The three offspring method

When we were describing the method we used to simulate a tilted square lattice, we mentioned that we took two cyclic permutations $\boldsymbol{\pi}, \boldsymbol{\pi}^*$ such that $\boldsymbol{\pi} \circ \boldsymbol{\pi}^* = \mathbb{1}$, and choose one of them at random to represent the bonds in any layer. Though this does represent a tilted square lattice, we the choice here seems to be unnecessary. Irrespective of the choices that we make at each layer we do get the same graph in the end. Hence, we can eliminate this step of the procedure where we make a choice and construct a graph where each element has three offspring:

1. One which it gets because of the permutation $\boldsymbol{\pi}$.

2. One which it gets because of the permutation $\boldsymbol{\pi}^*$.

3. One which it gets because of the identity permutation.

By the same logic, each element has three parent elements as well. The properties that we studied in the previous section can be studied for these graphs as well. Most of the

qualitative arguments presented in the previous section will follow through to this section as well.

Two offspring method   Three offspring method
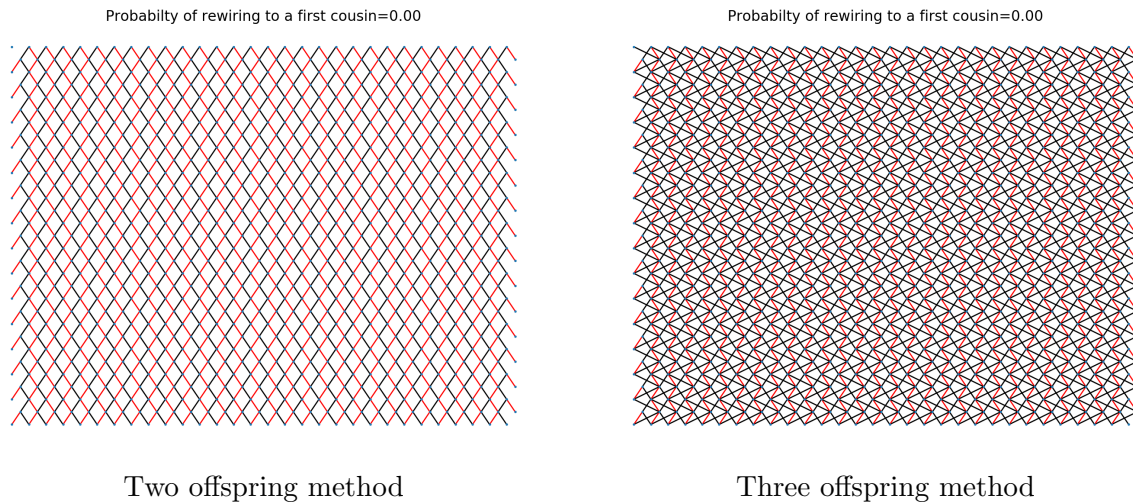
Figure 5.12: Graphs generated by the two methods. The identity permutations are represented by the red bonds.

5.2.1   Volume vs diameter for rewired causets
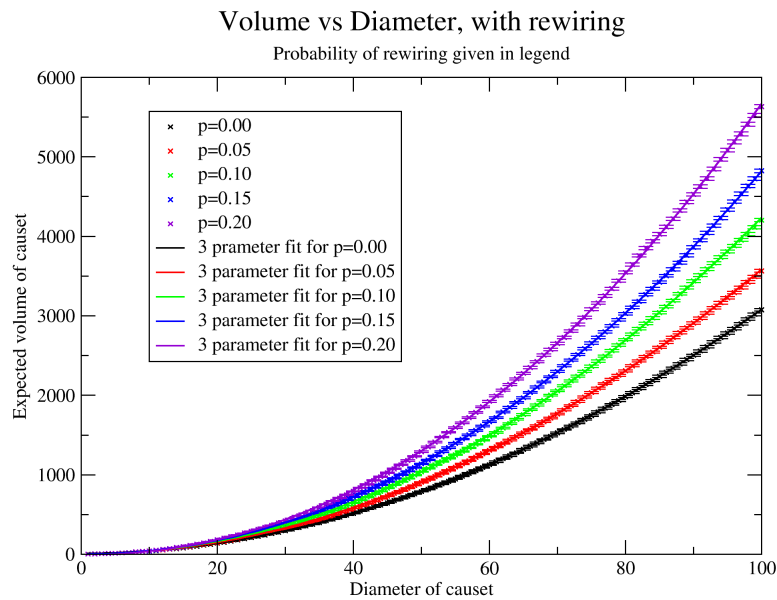
Figure 5.13: Volume vs diameter for after rewiring a lattice generated using the three offspring scheme. The three parameter fit was of the form $y = +a_0 + a_1 x^{a_2}$. $a_2 \sim 2$ for all the given curves.

Though the trends observed in this scheme are similar to that in the previous one, we can see that the actual volumes are greater. This is because the scheme has three children assigned to each element and we can have a greater 'spread' of the causets considered, due to this.

5.2.2 Volume distribution for various diameters

Figure 5.14: Volume distribution of rewired posets of different diameters. We can see the 'spreading out' of the individual volume peaks from $p_{\mathrm{rew}} = 0.00$ to $p_{\mathrm{rew}} = 0.20$

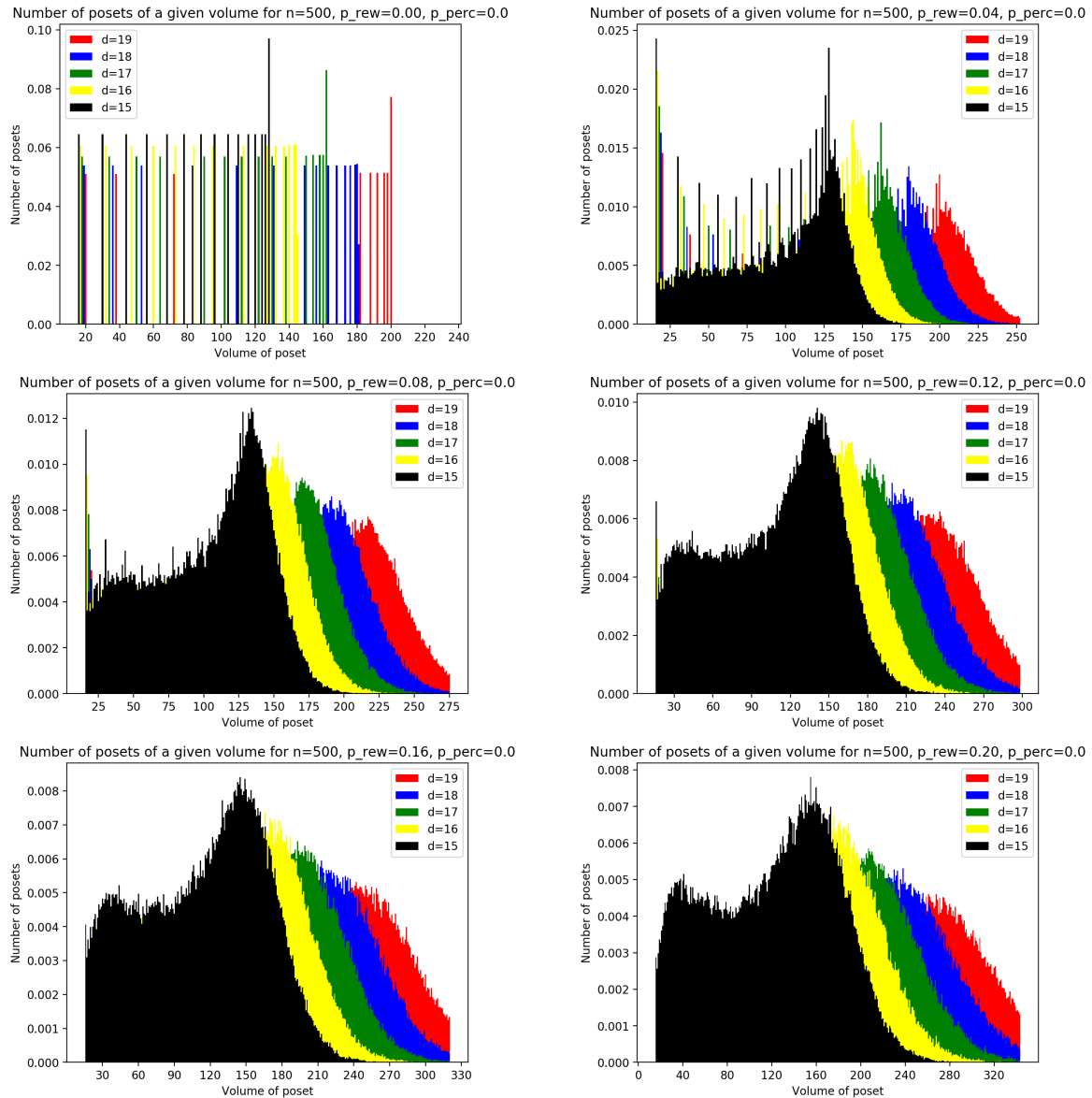We can see the 'spreading' of peaks as in the two offspring case, but there are a few differences. Though the number of peaks in the $p_{\text{rew}} = 0$ histogram is the same as that of the two-offspring case, the heights of these peaks are different. We see a much higher $V = k_2 d^2$ peak. With rewiring, the peak at $V = d + 1$ also gets diminished significantly. This is perhaps because of the high coordination number makes sure that two given elements very often have more than one path connecting them, making the $V = d + 1$ subcausets reasonably rare. Despite removing the initial $V = d + 1$ peak, we still have a graph which does not look quite like Figure 3.7.

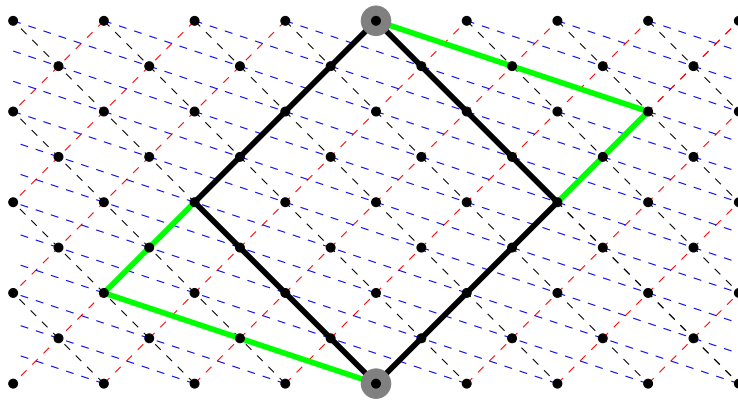Figure 5.15: Here we have an illustration to show how the three-offspring scheme affects the volumes of subcausets. The black square subcauset is contains the volume of the two-offspring case (whose bonds are represented by the red and black dashed lines). The green lines show us the volume which is added due to the other set of bonds which are added due the other permutation $\boldsymbol{\pi}^*$ (denoted by the blue dashed lines).

5.2.3 Volume *vs* probability of rewiring

Dependence of volume of causets on probability of rewiring

diameters of causets considered are given in the legend
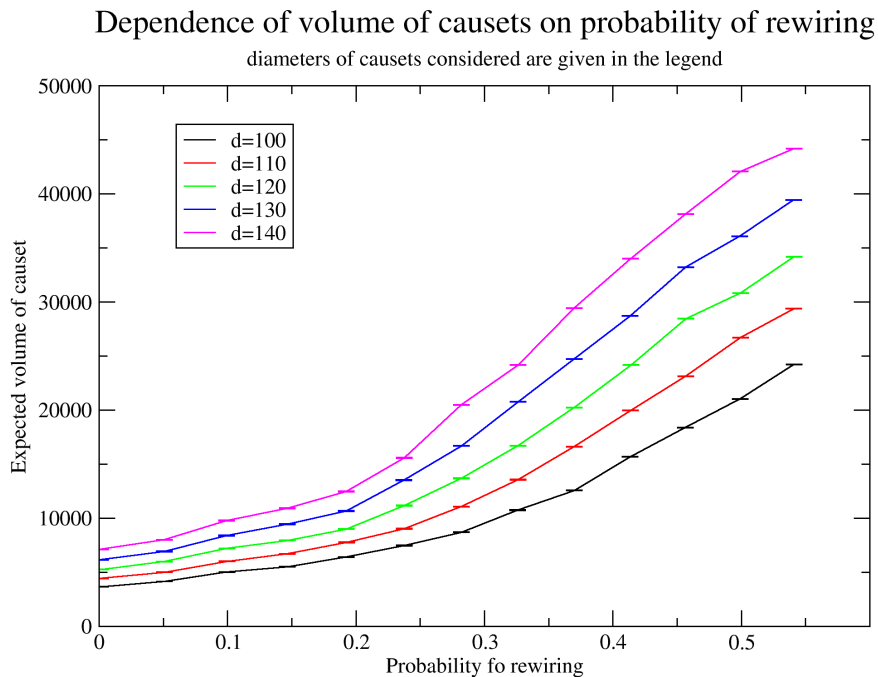
Figure 5.16: Volume *vs* probability of rewiring for different diameters. The simulation was done in a 200 layered causet, with three-offspring scheme.

Here again, we see the near linear increase in volume initially, before it shoots up. The shooting up is more apparent as the coordination number of these graphs are higher, and each productive rewiring will result in the addition of a greater volume than in the two-offspring case

5.2.4 Percolation on rewired graphs

If we study the causets that are formed by removing a finite fraction p_{perc} of the bonds in graphs generated by the three-offspring method, we do not see any new properties which we did not see in the two-offspring scheme.

Figure 5.17: Volume frequencies with percolation. $p_{\mathrm{rew}} = 0.16, 0.20$ and $p_{\mathrm{perc}} = 0.2$
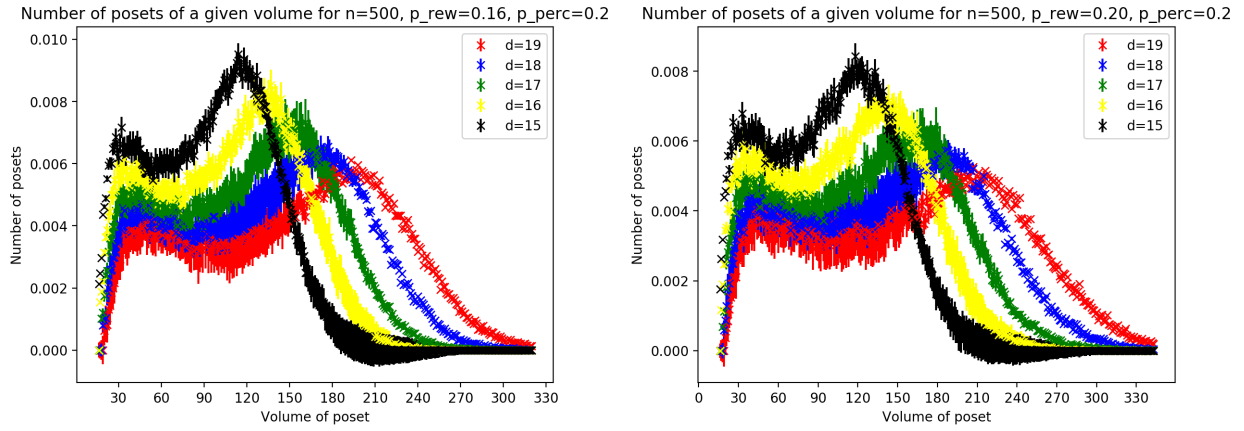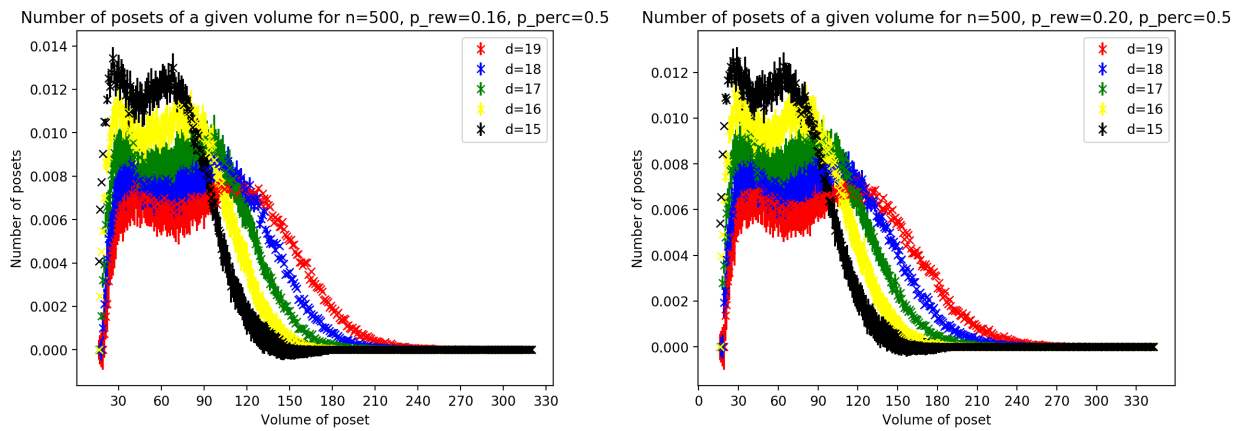

Figure 5.18: Volume frequencies with percolation. $p_{\mathrm{rew}} = 0.16, 0.20$ and $p_{\mathrm{perc}} = 0.5$

Chapter 6

Summary and directions for future work

We can attempt to find a scheme where we generate layered causets which have a Gaussian-like distribution in volumes as we saw in Figure 3.7. Though we did achieve a partial success with rewirings and percolation on a tilted square lattice, it is far from sufficient. We can also try to find a different scheme apart from this layered graph method, as properties such as Lorentz invariance, which we would like our causets to have, have been studied and one of the factors that are used to determine how good the causet is (with respect to Lorentz invariance) is how the longest path between two elements varies with respect to the shortest path between them. As a layered causet has no difference between the shortest and longest paths between two elements, Lorentz invariance is not something we have been able to verify in our causet. Rotational invariance is another property of spacetime which is obeyed by an ensemble average of Poisson sprinkled points. If we are able to match the properties of the causets generated by any scheme to those of causets generated by Poisson sprinkling, it would be reliable way to generate causets without using the crutch of a pre-existent spacetime manifold. We could possibly define a 'causal set action' for the scheme we choose, similar to the Benincasa-Dowker action, and we could attach an energy cost to "bad" causets so that "good" causets are selected. We could possibly construct a Metropolis algorithm to generate such causal sets using this action.

Bibliography

[1] Rafael D. Sorkin. "Forks in the road, on the way to quantum gravity". In: *International Journal of Theoretical Physics* 36.12 (Dec. 1997), pp. 2759–2781. ISSN: 1572-9575. DOI: `10.1007/bf02435709`. URL: `http://dx.doi.org/10.1007/BF02435709`.

[2] Luca Bombelli et al. "Space-time as a causal set". In: *Phys. Rev. Lett.* 59 (5 Aug. 1987), pp. 521–524. DOI: `10.1103/PhysRevLett.59.521`. URL: `https://link.aps.org/doi/10.1103/PhysRevLett.59.521`.

[3] S. W. Hawking, A. R. King, and P. J. McCarthy. "A new topology for curved space–time which incorporates the causal, differential, and conformal structures". In: *Journal of Mathematical Physics* 17.2 (1976), pp. 174–181. DOI: `10.1063/1.522874`. eprint: `https://doi.org/10.1063/1.522874`. URL: `https://doi.org/10.1063/1.522874`.

[4] David Finkelstein. "Space-Time Code". In: *Phys. Rev.* 184 (5 Aug. 1969), pp. 1261–1271. DOI: `10.1103/PhysRev.184.1261`. URL: `https://link.aps.org/doi/10.1103/PhysRev.184.1261`.

[5] E. C. Zeeman. "Causality Implies the Lorentz Group". In: *Journal of Mathematical Physics* 5.4 (1964), pp. 490–493. DOI: `10.1063/1.1704140`. eprint: `https://doi.org/10.1063/1.1704140`. URL: `https://doi.org/10.1063/1.1704140`.

[6] Geoffrey Hemion. "A quantum theory of space and time". In: *Foundations of Physics* 10.11 (1980), pp. 819–840. ISSN: 1572-9516. DOI: `10.1007/BF00708682`. URL: `https://doi.org/10.1007/BF00708682`.

[7] D. P. Rideout and R. D. Sorkin. "Classical sequential growth dynamics for causal sets". In: *Physical Review D* 61.2 (Dec. 1999). ISSN: 1089-4918. DOI: `10.1103/physrevd.61.024002`. URL: `http://dx.doi.org/10.1103/PhysRevD.61.024002`.

[8] David Rideout. *Dynamics of Causal Sets*. 2002. arXiv: `gr-qc/0212064 [gr-qc]`.

[9]   Tommaso Bolognesi and Alexander Lamb. *Simple indicators for Lorentzian causets.*
        2014. arXiv: `1407.1649 [gr-qc]`.

[10]   Sumati Surya. "The causal set approach to quantum gravity". In: *Living Reviews in
        Relativity* 22.1 (Sept. 2019). ISSN: 1433-8351. DOI: `10.1007/s41114-019-0023-1`.
        URL: `http://dx.doi.org/10.1007/s41114-019-0023-1`.

[11]   Béla Bollobás and Graham Brightwell. "Box-Spaces and Random Partial Orders". In:
        Transactions of the American Mathematical Society 324.1 (1991), pp. 59–72. ISSN:
        00029947. URL: `http://www.jstor.org/stable/2001495`.

[12]   Graham Brightwell and Ruth Gregory. "Structure of random discrete spacetime". In:
        Phys. Rev. Lett. 66 (3 Jan. 1991), pp. 260–263. DOI: `10.1103/PhysRevLett.66.260`.
        URL: `https://link.aps.org/doi/10.1103/PhysRevLett.66.260`.

[13]   D Kleitman and B Rothschild. "The number of finite topologies". In: *Proceedings of
        the American mathematical Society* 25.2 (1970), pp. 276–282.

[14]   Dionigi M T Benincasa, Fay Dowker, and Bernhard Schmitzer. "The random discrete
        action for two-dimensional spacetime". In: *Classical and Quantum Gravity* 28.10 (Apr.
        2011), p. 105018. DOI: `10.1088/0264-9381/28/10/105018`. URL: `https://doi.org/`
        `10.1088%2F0264-9381%2F28%2F10%2F105018`.

[15]   Dan Romik. *The Surprising Mathematics of Longest Increasing Subsequences.* Institute
        of Mathematical Statistics Textbooks. Cambridge University Press, 2015. DOI: `10.`
        `1017/CBO9781139872003`.

[16]   J.M. Hammersley. "A few seedlings of research". In: *Proceedings of the Sixth Berkeley
        Symposium on Mathematical Statistics and Probability, Volume 1: Theory of Statistics.*
        Berkeley, California: University of California Press, 1972, pp. 345–394.

[17]   SM Ulam and EF Beckenbach. "Modern Mathematics for the Engineer: Second Series".
        In: (1961).

[18]   Jinho Baik, Percy Deift, and Kurt Johansson. "On the distribution of the length of the
        longest increasing subsequence of random permutations". In: *Journal of the American
        Mathematical Society* 12.4 (1999), pp. 1119–1178.

[19]   Conrado Martínez, Alois Panholzer, and Helmut Prodinger. "Generating Random De-
        rangements". In: *Proceedings of the Meeting on Analytic Algorithmics and Combina-
        torics.* ANALCO '08. San Francisco, California: Society for Industrial and Applied
        Mathematics, 2008, pp. 234–240.

[20]   Sandra Sattolo. "An algorithm to generate a random cyclic permutation". In: *Information Processing Letters* 22.6 (1986), pp. 315–317. ISSN: 0020-0190. DOI: `https://doi.org/10.1016/0020-0190(86)90073-6`. URL: `http://www.sciencedirect.com/science/article/pii/0020019086900736`.